NUMERICAL SIMULATION OF THERMAL PERFORMANCE BASED ON COGENERATION LOW CARBON HEATING UNIT MANUFACTURING

by

Wei ZHOU*

Changzhou Vocational Institute of Mechatronic Technology,
Changzhou, Jiangsu, China

Original scientific paper
https://doi.org/10.2298/TSCI2402449Z

The renewable energy complementary cogeneration system has broad application prospects in the field of regional comprehensive energy utilization. The author proposes a trough solar assisted biomass cogeneration system, which uses medium and low temperature trough solar energy to heat conduction oil, drives absorption heat pump to preheat water in the heating network, saves heating steam extraction and increases power output under the condition that biomass fuel and heat supply remain constant. The EBSILON professional software was used to model and simulate the case unit and integrated system, and based on this, thermodynamic characteristics such as system energy flow and energy loss were analyzed. The results indicate that: under the design condition, 1.78 MWh of solar power can be generated, the photoelectric efficiency is 20.06%, and the photoelectric conversion efficiency can reach 21.60%. Hourly simulation analysis of the whole heating season shows that the total solar power generation generated in five months of the heating period is 1124.30 MWh, and the average photoelectric efficiency is 16.49%.

Key words: *trough solar energy, biomass cogeneration, absorption heat pump, system integration, thermodynamic analysis*

Introduction

Energy is the engine of human society's progress. The exploitation of energy, especially the overexploitation of primary energy represented by coal, has led to the reduction of non-renewable resource. At the same time, environmental pollution issues that affect human survival are also closely related to energy production. In order to develop low carbon economy, the gas steam combined cycle unit using clean natural gas is a more environmentally friendly power generation method. The application of clean and efficient combined cycle in cogeneration is of great significance for improving energy efficiency. With the launch and implementation of China's *West-East Gas Pipe-line* project, combustible ice resources in the South China Sea and the *two engines* (aero engines and heavy gas turbines) project, clean and efficient gas turbines and their combined cycle will be conducive to the future growth of China's clean energy. Most industrial developed countries mainly consume oil and natural gas in primary energy, which is also the basis for the development of gas turbines and their combined cycle worldwide [1]. China's energy consumption is mainly coal. However, with the further promotion of low

* Author's e-mail: w1003zhou38@sina.com

carbon economy, the demand for gas turbines and their combined cycle will become stronger and stronger.

Firstly, in general, the difference between the peak and valley load values of each inter provincial power system is about 30-40% of the maximum load, and even exceeds 50% during peak hours. This phenomenon is particularly severe in large and medium-sized cities, which requires stricter peak shaving requirements for units. At the same time, in order to absorb different types of renewable energy, there are more new requirements for the regulation of power grid energy. Gas turbines and their combined cycles have the characteristics of fast start-up, good peak shaving, and short construction cycles, which are one of the effective ways to solve the aforementioned contradictions [2]. Facts have proven that the future of China's power industry has a place for gas turbine combined cycle. Secondly, due to the increasingly severe environmental pollution, the demand for environmental protection is becoming increasingly strong, creating conditions for the use of clean and efficient gas turbines in China. Based on the *Air Pollution Prevention and Control Law*, China implemented strict *Air Pollution Emission Standards for Thermal Power Plants* nationwide in 2012. Under the conditions of allowing natural gas resource reserves, replacing coal-fired power plants with gas turbine combined cycle power plants not only saves energy, but also reduces environmental pollution in central cities in the simplest and most effective way. The newly introduced environmental protection tax law in 2018 has played a positive role in promoting China's environmental protection.

In addition, high end engines centered around gas turbines are an important manifestation of a major country's core manufacturing capabilities. Since the beginning of the 21st century, China has introduced 100 MW E-type units from GE and Alstom, and built a number of gas-fired power stations. Among them, the vast majority are combined cycle power plants, and currently more than 70 power plants have been put into operation. Since 2003, China has introduced F-class large gas turbines from General Electric, Siemens, and Mitsubishi Heavy Industries, its single unit power is about 260-280 MW, and the combined cycle single unit power can reach 390-400 MW, with a cycle efficiency of 57-58%. In recent years, due to various factors such as energy conservation, environmental protection, and urban heating, many cities have begun to build gas turbine power plants. According to the goals set in the 13th Five Year Plan for gas turbine technology, by 2023, China will break through key technologies in the design, component manufacturing, and operation and maintenance of heavy-duty gas turbines.

Literature review

Cogeneration (CHP) technology is an important measure to achieve energy conservation and emission reduction in the power generation industry. Large capacity, high parameter coal-fired CHP units have been built and put into operation in batches, and the installed capacity ranks second in the world. At present, *heat to electricity* is the main operating mode of coal-fired CHP units. In recent years, the country has vigorously promoted the grid connection of clean energy power generation such as wind and photovoltaic, resulting in a large number of CHP units often operating at lower loads or even shutting down during non-heating seasons, making it difficult to meet external heat demand under the *heat to electricity* operating mode. In addition, according to their own process requirements, industrial users have fixed heat consumption parameters. When the industrial hot steam pressure is higher than the exhaust pressure of the intermediate pressure cylinder of the steam turbine, the commonly used steam extraction heating method of the steam turbine will have a negative impact on the CHP unit equipment, thereby limiting the unit's ability to provide external heating. In contrast, T describes the thermal and radiative effects associated with FCM fuels, as well as the effects of

different heat transfer rates. The research results can provide recommendations for better development and forecasting of FCM oils [3]. Hussain *et al*. [4] performed a sensitivity analysis on four different scenarios. Thermal performance of building materials, permeability, function, time, light and glass selection are based on spatial research. The results show that the indoor thermal quality of a school affects its thermal performance and future heating and cooling energy needs. Boldoo, T analyzed the thermal performance of single-phase absorption refrigeration systems (ARS) using 1-hexyl-3-methylimidazolium (HMIM) cationic ionic liquid and different MWCNT nanoparticles supporting R1234yf refrigerant. The specific heats of various MWCNT nanoparticle-reinforced [HMIM] cationic ionic liquids were obtained at 303-383 K and 0-1 wt.%, respectively, and then used in solubility and adsorption cooling cycle models. As a result, the highest specific heat of all identified ionic liquids was detected at the highest temperature of 383 K [5].

Based on the previous background, the author proposes a trough solar assisted biomass cogeneration system, which collects heat from the solar radiation and is used to drive the absorption heat pump to preheat the water in the heating network, save heating and steam extraction get more power generation. Through power analysis and thermodynamic state analysis, the fundamental reason for improving system performance is revealed. In addition, the daily and annual performance of the integrated system is also discussed, which can provide theoretical guidance for the research and practical application of solar energy and biomass energy in the integrated system of cogeneration.

Numerical simulation of thermal performance

Case unit introduction

The author chose a biomass cogeneration plant in northwest China as a reference material, and the flow system is shown in fig. 1. The heat generator and pressurizer fed from the biomass boiler operated by the generator condense and then enter the condenser three-stage low heater, deaerator, and two-stage high heater, respectively. During the local heat supply period (151 days from November 1st to March 31st of the following year), three units are extracted for the purpose of heating the heating network of the heat network and provide heat to the local people.

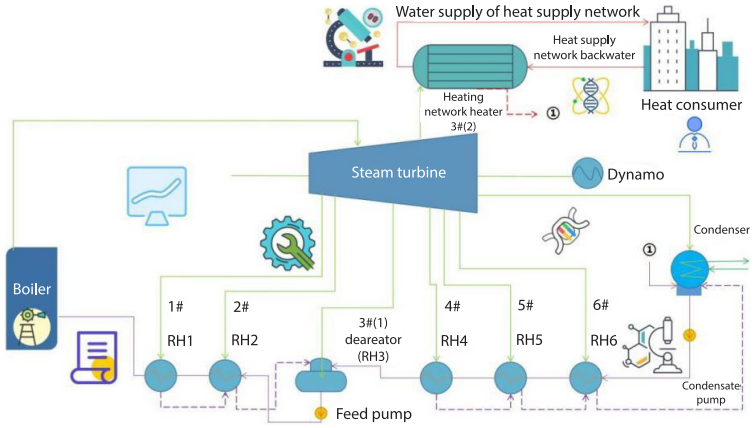

Figure 1. Schematic diagram of a biomass unit in a case study

Tables 1 and 2, respectively list the basic parameters of the case unit and its regenerative system. During the heating period, 4.46 kg per second of 3# steam extraction is used for regional heating, heat the 73.80 kg per second return water of the heating network from 49.9-

99.3 °C, providing 14.28 MWh of heat to the heat users. The net power generation generated at the same time is 29.98 MWh, and the biomass consumption is 11.82 kg per second. The main raw materials for biomass boilers are corn straw, corn cob, rice straw, and rice husk, with an average low calorific value of 9.435 MJ/kg for fuel.

Table 1. Case – basic thermodynamic parameters of biomass units

Parameter	Main steam pressure [MPa]	Main steam temperature [°C]	Main steam flow rate [kgs^{-1}]	Exhaust pressure [kPa]	Exhaust temperature [°C]	Exhaust flow rate [kgs^{-1}]	Boiler efficiency [%]
Numerical value	9.40	545.0	37.89	4.90	33.5	21.20	89.0

Table 2. Case – basic paramete-rs of heat recovery system of biomass unit

Parameter	RH1	RH2	RH3	RH4	RH5	RH6
Extraction temperature [°C]	391.4	312.9	278.1	182.8	120.8	85.4
Extraction pressure [MPa]	2.75	1.44	1.13	0.37	0.17	0.06
Extraction flow rate [kgs^{-1}]	2.28	1.37	7.02	1.43	1.73	2.34
Drainage temperature [°C]	193.4	165.7	–	116.0	84.7	31.5
Drainage flow rate [kgs^{-1}]	2.28	4.07	–	1.43	3.15	5.60
Outlet feedwater temperature [°C]	219.3	187.8	160.1	143.0	109.4	79.1
Outlet feedwater flow rate [kgs^{-1}]	38.89	38.89	38.89	33.35	33.35	33.35

System modelling and simulation

System Modelling. It maintains balance among components, subsystems, and the entire system while ensuring mass and energy conservation. In this software, the thermodynamic cycle is constructed from the non-linear equations, solved by a series of linear equations iteratively, and the variable coefficient is formed by using the iterative value of the previous step. When the basic variable is no longer changed, the iteration stops. After verification, this software is a reliable thermodynamic modelling software [6]. Based on the boundary conditions of the case unit, a model was established using the built-in module of EBSILON Professional, and the calculation results were compared and analyzed with the design data of the case unit. The results showed that the simulation model was accurate and reliable.

System integration. In order to improve the utilization rate of solar energy and use more renewable energy to generate electricity and heat, the author proposes a trough solar assisted biomass cogeneration system. First, the heat transfer oil from the solar collector acts as a thermal guide and releases the heat in the heat pump generator. The circulating working fluid absorbs heat and evaporates, and gas is formed in the condenser of the heat pump. After adjustment, it flows to the evaporator. Second, the low power device of the evaporator takes some heat to transfer to the cold water, the gas absorbs the heat from the cold water, and the water evaporates. Finally, the moist room is kept below temperature and sent to vacuum for absorption with lithium bromide solution. Therefore, the heat produced by the heat pump in the suction and condenser can be used to preheat the water in the heating network. After that, the water in the heating network is heated to the required level by 3 minus units in the heating network heater.

Solar thermal system parameters

The solar thermal system adopts the Eurotrough ET-150 commercial parabolic trough collector, which uses 12 collector components. The circulating working fluid uses Thermol VP-1 thermal oil, which is pressurized by a thermal oil pump and sent to an absorption heat pump.

Evaluation indicators

Energy evaluation index based on First law of thermodynamics. It is defined as the ratio of total energy output to total energy input, which represents the degree of energy conversion of the integrated system. It can be calculated:

$$\eta_t = \frac{P_{e,t} + Q_{h,t}}{Q_b + Q_s} \tag{1}$$

where $P_{e,t}$ is the net total power generation, $Q_{h,t}$ – the net total heating capacity, Q_b – the input energy of biomass fuel, and Q_s – the input energy of solar energy [7].

The input energy Q_b of biomass fuel and the input energy Q_s of solar energy are calculated:

$$Q_b = Q_{\text{LHV}} m_b \tag{2}$$

$$Q_s = \frac{I A_{SF}}{1000} \tag{3}$$

where Q_{LVH} is the low calorific value of biomass fuel, m_b – the amount of biomass fuel, I – the intensity of direct normal radiation (DNI) from the Sun, and A_{SF} – the effective optical area of the mirror field.

Due to the constant heating capacity of the integrated system and the case unit, the additional electricity generated by the system after the introduction of solar energy can be considered as solar power generation. For integrated systems, solar power generation can be expressed:

$$P_{e,s} = P_{e,t} - P_{e,b} \tag{4}$$

where $P_{e,b}$ is the biomass power generation, which remains unchanged before and after integration. The photoelectric efficiency $\eta_{en,s}$ is used to evaluate the utilization rate of collected solar energy:

$$\eta_{en,s} = \frac{P_{e,s}}{Q_s} \tag{5}$$

The average photoelectric efficiency $\eta_{en,s}$ in heating season is used to measure the utilization rate of solar energy collected in the whole heating season, which can be calculated:

$$\eta_{en,s,a} = \frac{\sum_{k=1}^{3624} P_{s,k}}{\sum_{k=1}^{3624} Q_{s,k}} \tag{6}$$

Shed evaluation index based on Second law of thermodynamics. The total conversion efficiency $\eta_{en,s}$ is often used to measure the degree of utilization of system resources:

$$\eta_{en,t} = \frac{E_e + E_h}{E_b + E_s} \tag{7}$$

where E_e is the net power output, E_h – the net heating output, E_b – the input of biomass fuel, and E_s – the input of solar energy. Among them, E_b and E_s can be calculated:

$$E_b = Q_b \left[1.044 + 0.016 \frac{\omega_H}{\omega_C} - 0.3493 \frac{\omega_O}{\omega_C} \left(1 + 0.0531 \frac{\omega_O}{\omega_C} \right) + 0.0493 \frac{\omega_N}{\omega_C} \right] \Bigg/ \left(1 - 0.4124 \frac{\omega_O}{\omega_C} \right) \tag{8}$$

$$E_s = Q_s \left[1 - \frac{4}{3} \left(\frac{T_0}{T_s} \right) + \frac{1}{3} \left(\frac{T_0}{T_s} \right)^4 \right] \tag{9}$$

$$\eta_{ex,s} = \frac{P_{e,s}}{E_s} \tag{10}$$

Result analysis

The integrated system was simulated using EBSILON Professional software, and the basic parameters of the solar thermal system in the design scheme are shown in tab. 3. Choose 15:00 p. m. on March 21st as the design point for the integrated system, at which time the DNI is 908.67 W/m^2 and the mirror field efficiency is 51.18%. The heat transfer oil absorbs heat from 123.0-153.0 ℃ in the collector and is used to drive the absorption heat pump. The circulating cooling water entering the absorption heat pump is cooled from 27.4-25.5 ℃. The water supply of heat supply network obtained 8.22 MWh of heat from conduction oil and circulating cooling water, the temperature increased from 49.9-75.2 ℃, and the COP of absorption heat pump reached 1.766. The basic parameters of the absorption heat pump are shown in tab. 4.

Table 3. Basic parameters of the solar thermal system

Parameter	DNI [Wm^{-2}]	Heat transfer oil inlet (outlet) temperature [℃]	Heat transfer oil flow rate [kgs^{-1}]	Solar input [MWh]	Mirror field efficiency [%]	Effective energy [MWh]
Numerical value	908.67	122.0(153.0)	87.37	8.89	51.18	4.64

Table 4. Basic parameters of absorption heat pump

Parameter	Numerical value
Heat transfer oil inlet (outlet) temperature [℃]	153.0 (123.0)
Heat transfer oil flow rate [kgs^{-1}]	82.37
Cooling water inlet (outlet) temperature [℃]	27.4 (25.5)
Cooling water flow rate [kgs^{-1}]	413.67
Heat supply network water inlet (outlet) temperature [℃]	49.9 (75.2)
Heating network water flow rate [kgs^{-1}]	77.82
Heating capacity [MWh]	8.22
COP	1.766

Due to the use of solar thermal systems to assist in heating during the heating season, the parameters of the heating network heater in the integrated system have changed compared to before. Table 5 lists the comparison of the parameters of the heating network heater in the

case unit and the integrated system. In the integrated system, the heating network water supply is preheated in the absorption heat pump before entering the heating network heater, and the water temperature rises from 49.9-75.2 °C. Therefore, the steam extraction volume of 3# entering the heating network heater significantly decreased from 4.46-1.98 kg per second, and the thermal load of the heating network heater decreased by 8.23 MWh, a decrease of 53.49% compared to before.

Table 5. parameter comparison of heat net heater in case unit and integrated system

parameter	Case unit	Integrated system	*D*-value
Inlet temperature of heating network water supply [°C]	49.9	75.2	25.3
Outlet temperature of heating network water supply [°C]	99.3	99.3	0
Heating network water supply flow rate [kgs^{-1}]	73.80	73.80	0
Heating extraction pressure [MPa]	3.12	2.12	1
Heating extraction temperature [°C]	287.1	287.1	0
Heating extraction flow rate [kgs^{-1}]	4.46	1.98	-2.48
Heating and drainage temperature [°C]	60.0	85.2	25.2
Heating and drainage flow rate [kgs^{-1}]	4.46	1.98	-2.48
Heating load of heating network heater [MWh]	14.28	6.05	-8.23

Compared with the unit in the case, the performance of the unit in the integrated system has been greatly improved on the premise that the biomass fuel volume remains the same. The heat supply of the integrated system is still 14.28 MWh, while the net power generation has increased by 5.94%. Due to the introduction of solar energy, the total energy conversion efficiency has decreased by 1.52%, and the photoelectric efficiency can reach 20.06%.

Since the biomass energy is stable, the standard value is set at 100. Also, the flow and temperature of the return water and supply water of the heating network do not change before and after integration, so the heat can be constant. Compared to the model where only three extraction devices are used to heat water for district heating, mixed systems use heat pumps and district heating to heat district heating water. The heat exchanger receives 4.63 MWh of solar energy, which is used to drive the heat pump [8]. The circulating cold water acts as a low temperature heat source, releasing 3.60 MWh of energy to the heat pump. So, if the water heat network absorbs 8.23 MWh of heat from the heat pump, the energy absorbed by the heat network will decrease by 8.23 MWh, and the required three extractions will decrease by 2.48 kg per second unit price. So, if the thermal capacity is maintained, the total electricity production has increased by 2.02 MWh, and the electric power has increased by 1.78 MWh.

In order to further explore the root cause of the improvement in unit performance caused by the integration solution, a comprehensive analysis was conducted on the case unit and integrated system. Before and after integration, the input of biomass fuel remains constant (considered as 100%), and the losses of biomass boilers remain unchanged. The 8.25 MWh of solar energy is input into the integrated system, and the exhaust steam increases with the decrease of heating and extraction steam, resulting in increased losses for steam turbines, condensers, and generators.In addition, due to the auxiliary heating of the solar thermal system,

the heat loss of the heating network heater is reduced by 1.76 MWh, while the heat loss of the solar thermal system is 7.34 MWh. Overall, the power loss of the entire system has increased by 6.48 MWh. Meanwhile, the total output has increased by 1.78 MWh. Although the overall efficiency has decreased by 0.22%, the photoelectric conversion efficiency can reach 21.60%. The non-heating period in the local area is from April 1st to October 31st each year. The absorption heat pump and heating network heater stop working, and the system uses the traditional solar assisted heating water supply pure condensation power generation mode to operate [9]. At this time, the heat transfer oil enters the feed water heater to heat part of the feed water to the outlet water temperature of RH1. Therefore, the extraction steam of 1# and 2# is reduced, and the saved extraction steam can continue to expand and work in the turbine, resulting in an increase in total power generation. Evaluate the performance of typical meteorological years during non-heating periods, and the monthly performance analysis results are shown in fig. 2.

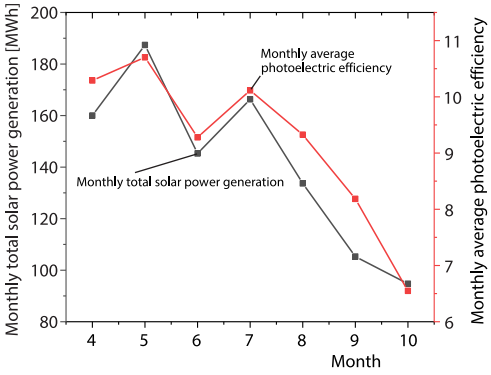

Figure 2. Monthly performance of the solar thermal system in the typical annual non-heating season

It can be seen that in the non-heating period, the best performance of the system is in May. After adopting the solar thermal system, the power generation has increased by 190.80 MWh, and the monthly average photoelectric efficiency is 10.63%. Considering the whole non-heating period, the total amount of solar power generation can reach 995.87 MWh, and the average photoelectric efficiency is 9.24%. Compared to the heating period, the system performance during non-heating period is poor, which is related to the solar incidence angle and the temperature of thermal oil utilization, thus demonstrating the superiority of the solar assisted power generation technology proposed by the author during heating period.

Conducting economic analysis on the aforementioned solar thermal system, the cost and benefits of the biomass unit remain consistent before and after integration. The new revenue is the benefits brought by solar assisted power generation, and the new expenses include initial investment and operation and maintenance costs. Among them, the increased equipment mainly includes solar collectors, absorption heat pumps and feedwater heaters [10]. The total area of the collector is 10368 m^2, which is approximately 3.5 times the total area of the collector. The main economic parameters adopted by the author are shown in tab. 6.

Table 6. Economic parameters of the solar thermal system

Parameter	Numerical value
Unit cost of collector [Yuan per m^2]	1400.00
Initial investment of absorption heat pump [10000 Yuan]	445.63
Initial investment of feedwater heater [10000 Yuan]	28.79
Land unit cost/collector unit cost	0.012
On grid electricity price [Yuan per kWh]	1.19
Annual operating and maintenance costs/total initial investment	0.01
Discount rate [%]	7.00

According to the aforementioned calculation, the total initial investment of the solar thermal system is 19.979 million Yuan, of which the investment in the solar collector is 14.5152 million Yuan, accounting for 72.65% of the total investment. A total of 2120.17 MWh of new electricity generation was added throughout the year, which can bring an additional benefit of 2.5442 million Yuan. The dynamic investment pay-back period is 12.3 years.

Conclusion

Utilizing solar energy to heat conduction oil as a high level heat source, driving an absorption heat pump to preheat the heating network for water supply, saving steam turbine heating and extraction increase net power generation. The main conclusions are: After the system integration, although the biomass fuel quantity and heat supply quantity remain unchanged, 1.78 MWh of solar power can be generated under the design condition, with the photoelectric efficiency of 20.06% and the photoelectric conversion efficiency of 21.60%. In non-heating seasons, the system uses the pure condensing power generation mode of solar assisted heating water supply, and the total solar power generation can reach 995.87 MWh, with an average photoelectric efficiency of 9.24%. The total initial investment of the solar thermal system is 19.979 million Yuan, which can bring additional benefits of 2.5442 million Yuan per year. The dynamic investment pay-back period is 12.3 years.

References

[1] Yu, D., Li, H., Numerical Simulation of Thermal Performance of Gaas-Metal-Organic Chemical Vapor Deposition Reactor Based On 36 × 4 Inches' Wafers, Crystal Research and Technology, *Journal of Experimental and Industrial Crystallography*, *96* (2022), 5, 57
[2] Xue, D., *et al*., Prediction of Structural Mechanical Properties of Energy-Saving Materials for Solar Photovoltaic Photo-Thermal System Based on Deep Learning, *Thermal Science*, *27* (2023), 2B, pp. 1109-1116
[3] Changbing, T., *et al.*, Numerical Simulation Research on the Irradiation-Thermal-Mechanical Performance Evolution of Fcm Fuel, *Frontiers in Energy Research*, *9* (2021), 1, 664345
[4] Hussein, M. H., *et al*., Effect of Thermal Mass of Insulated and non-Insulated Walls on Building Thermal Performance and Potential Energy Saving, *Journal of Physics: Conference Series*, *2042* (2021), 1, 012159
[5] Boldoo, T., *et al*., Numerical Investigation on Thermal Performance of Absorption Refrigeration System Using Mwcnt Nanoparticle-Enhanced 1-hexyl-3-methylimidazolium Cation-Based Ionic Liquids, *Applied Thermal Engineering: Design, Processes, Equipment, Economics*, *967* (2022), 206, 206
[6] Wang, X., *et al*., Numerical Simulation of End Face Heating in Alternating Current Flash Butt Welding Based on Electrical-Thermal Bidirectional Coupling, *The International Journal of Advanced Manufacturing Technology*, *69* (2022), 1-2, 120
[7] Zhao, D., *et al*., A Thermal Comfort and Peak Power Demand Aware VRF Heating/Cooling Management Framework: Simulation and on-Site Experiment, *Journal of Information Processing*, *30* (2022), 1, pp. 476-485
[8] Zhang, S., *et al*., Modelling and Optimal Control of Energy-Saving-Oriented Automotive Engine Thermal Management System, *Thermal Science*, *25* (2021), 4B, pp. 2897 - 2904
[9] Ettaieb, K., *et al*., A Flash-Based Thermal Simulation of Scanning Paths in LPBF Additive Manufacturing, *Rapid Prototyping Journal*, *654* (2021), 7, pp. 98-103
[10] Zhang, H., Electromagnetic Compatibility Analysis of Thermal Energy Recovery Power System Driven by New Energy Vehicles, *Thermal Science*, *27* (2023), 2A, pp. 1167-1174

Paper submitted: March 28, 2023
Paper revised: July 2, 2023
Paper accepted: September 27, 2023